Lessons from a Challenging System: Accurate Adsorption Free Energies at the Amino Acid/ZnO Interface

Lessons from a challenging system: accurate adsorption free energies at the amino acid / ZnO interface

Monika Michaelis,[†,‡] Massimo Delle Piane,[*,†,¶] Dirk Rothenstein,[§] Carole C. Perry,[‡] and Lucio Colombi Ciacchi[†]

†*Hybrid Materials Interfaces Group, University of Bremen, Faculty of Production Engineering, Bremen Center for Computational Materials Science, Center for Environmental Research and Sustainable Technology (UFT), and MAPEX Center for Materials and Processes, Am Fallturm 1, 28359 Bremen, Germany*

‡*Biomolecular and Materials Interface Research Group, Interdisciplinary Biomedical Research Centre, School of Science and Technology, Nottingham Trent University, Clifton Lane, Nottingham NG11 8NS, United Kingdom*

¶*Department of Applied Science and Technology, Politecnico di Torino, 10129 Torino, Italy*

§*Institute for Materials Science, Department of Bioinspired Materials, University of Stuttgart, Heisenbergstrasse 3, 70569 Stuttgart, Germany*

E-mail: massimo.dellepiane@hmi.uni-bremen.de

Abstract

We undertake steps to overcome four challenges that have hindered the understanding of ZnO/biomolecule interfaces at the atomic scale; parametrization of a classical force field, ZnO surface termination and amino acid protonation state in methanol, and convergence of enhanced- sampling molecular dynamics simulations. We predict adsorption free energies for histidine, serine, cysteine and tryptophan in remarkable agreement with experimental measurements obtained via a novel indicator-displacement assay. Adsorption is driven by direct surface/amino-acid interactions mediated by terminal hydroxyl groups and stabilized by strongly-structured methanol solvation shells.

1 Introduction

Interactions between biomolecules and inorganic materials are attracting growing attention in fields ranging from pharmaceutics to the development of novel materials.[1–3] Both naturally occurring and *de novo* synthesized biomolecules are known to recognize and bind to a wide range of metal, functional oxide, mineral, and polymer surfaces.[4] Individual amino acids and peptides are able to interact with materials with relatively high affinity and specificity, resulting in the generation of a strongly bound interface between the constituents.[5–8]

Over the past few decades, many experimental approaches have been developed to quantify biomolecule adsorption on materials' surfaces. These include adsorption isotherms, isothermal titration calorimetry (ITC), quartz crystal microbalance (QCM), surface plasmon resonance spectroscopy (SPR), single molecule force spectroscopy (SMFS), and fluorescence-based binding assays.[4] However, the free energy values estimated via these techniques provide no information on the molecular mechanisms giving rise to selective binding. This prevents a predictive transferability of the binding principles to other biomolecule-material systems.

Not only have we yet to achieve a valid and predictive description of how larger biomolecules interact with inorganic materials; even a fundamental understanding of individual amino acid/surface interactions remains poor. This is mainly because very few direct experi-

mental approaches are able to determine the atomistic details of such interfaces. In this context, atomistic simulations can be of great help, being able to provide both a quantitative and mechanistic description of adsorption at a molecular resolution. In the case of biomolecule/surface interactions in liquid solvents, the system size and complexity often require a molecular-mechanics description to keep the computational effort within reasonable limits, adding a layer of approximation that needs to be properly appraised.[9]

We identify here four different challenges that we believe impact on the predictive power of such simulations: 1. the availability of an accurate force field, 2. the action of the solvent, particularly on the physical and chemical features of the surface, 3. the chemical states of the biomolecules, particularly their protonation/deprotonation in non-aqueous environments and 4. the method used to adequately sample the phase-space and compute adsorption free energies. In this work, we undertake steps to assess these challenges for the case of selected amino acids in interaction with the Zn $(10\bar{1}0)$ surface of zinc oxide.

ZnO wurtzite crystals are dominated by four low Miller index surfaces. In particular, the two non-polar surfaces (including $(10\bar{1}0)$) provide around 80% of the surface present in nano-structures under wet conditions at room temperature.[10] ZnO nanostructures are important materials in the area of bio-nano-combinatorics, due to their peculiar properties[11] and high abundance.[12] The morphology-dependent properties of ZnO can be altered using biomolecules. Amino acids have been used directly both as structure-directing agents during biomineralization of ZnO and for band-gap engineering,[13,14] leading to enhanced photocatalytic activity.[15] Different synthesis routes have been applied during such biomineralization studies,[16] employing for instance methanol as a solvent.[3]

We show in this study how adsorption free energies and binding configurations can be computed in accurate agreement with experimental measurements when all four challenges listed above are addressed. Firstly, accuracy depends on the quantitatively correct parameterization of the classical potentials (force fields) used to describe interactions at the hybrid bio-inorganic interface. While accurate and extensively validated force fields for biomolecules

have been available for some time,[17,18] force fields for oxide surfaces are still in their infancy.[19] In particular, very few are available to reliably describe hybrid bio-inorganic systems,[19,20] with some contributions coming from our own work.[21–24] Such force fields should be designed to straightforwardly work together with the most commonly employed biomolecular force fields, without any ad-hoc modification, to guarantee compatibility, simplicity and transferability to other material/biomolecule systems.

For biomolecule/ZnO systems, many subtle effects dictate the features of the interface. A delicate balance of competitive interactions among surface, biomolecules, and solvent needs to be properly considered in the simulation setup. In particular, the solvent plays a major role in controlling biomolecular adsorption.[25,26] Surface reconstruction caused by the solvent is known to strongly affect the strength of the interaction.[25] However, a careful consideration of the surface reconstruction by the solvent is often neglected in the simulation of biomolecule/material interfaces[27] and difficult to achieve, often due to the lack of compelling evidence coming from the experimental side.

For ZnO, for example, while empirical potentials have been devised and employed to study either its interaction with water[28] or amino acids,[27] no example exists in which both elements have been considered at the same time. In this regard, the known usage of different solvent environments for the synthesis of ZnO bio-composites further complicates the matter, with scarce information available about the surface termination in non-aqueous solvents, such as methanol. Additionally, the protonation state of biomolecules in such environments is still mostly unknown and needs to be evaluated on a case-by-case basis.

Finally, getting accurate binding free energies from molecular simulations necessarily relies on biasing the system dynamics, via so-called enhanced-sampling techniques, in order to overcome the sampling issues of standard molecular dynamics.[29] Many approaches have been chosen to study biomolecular adsorption, generally based on different flavors of either umbrella sampling or metadynamics.[30] It is beyond the scope of this article to give an overview of such methods and their advantages and limitations. However, it is important

to highlight here how their successful application is strongly dependent on the nature of the studied system. Particularly, the affinity of the solvent to the surface significantly affects their performance,[30] leading to the need for specific modifications to overcome this issue.[31,32]

A proper assessment on the validity of the simulation approach requires trustworthy experimental data that match as close as possible the conditions reproduced in the model. For this purpose, we recently developed a novel optically-sectioned planar-format indicator-displacement assay (O-IDA), which provided the first free energy values for the interaction of amino acids with specific crystal planes of ZnO in a methanol environment.[33] A methanol solvent was used to avoid the partial dissolution of these substrates in water.[34]

In this work, we expand these experiments and use the data as a validation basis for our simulations. We present a joint experimental/computational approach to characterize the adsorption of selected amino acids (histidine, cysteine, serine, tryptophan) on ZnO $(10\bar{1}0)$. Employing enhanced-sampling simulations based on metadynamics, made possible by the development of a bio-compatible force field for ZnO, we provide theoretical adsorption free energies and binding configurations. These are compared with the experimental measurements determined by the O-IDA approach. Additionally, we investigate solvent (water vs. methanol) and surface termination effects on the interaction, as steps towards the development of more realistic interface models. Our broader aim is to provide a collection of data and computational machinery essential to set-up a rational design platform for ZnO-based bio-nanocomposites, connecting the material's properties with the efficiency of its bio-functionalization.

2 Materials and Methods

2.1 Optically sectioned planar format indicator displacement assay (O-IDA)

To determine the binding affinities of the investigated amino acids, a fluorescence-based indicator displacement assay was applied in accordance with Michaelis et al..[33] Briefly, single-crystalline $(10\bar{1}0)$ ZnO substrates (Crystal GmbH, Berlin, Germany) were fixed in a 96 well plate after 30 min cleaning treatment with an UV Ozone Cleaner (ProCleaner Plus, BioForce nanosciences). First, a 10 μM FluoZin-1 Dye (F24181, Thermo Fisher) solution in methanol was prepared and 200 μl incubated with the ZnO single crystals for 2 h on a plate shaker (mini orbital shaker SSM1, Stuart, 30 rpm) at room temperature (RT). The dye-containing solution was removed and replaced with 200 μl of methanol (control) or with 200 μl of solutions (1 nM to 1 mM) containing the test compound (Trp, Sigma-Aldrich) and incubated (2 h) using the same conditions as above. The fluorescence of FluoZin-1 was measured with a confocal laser scanning microscope (Leica TCS SP5, Leica microsystems) using the 496 nm laser line for excitation and the detection of fluorescence between 498 nm and 601 nm along the z-axis at RT. We used Leica HCX PL Fluotar objectives (10×), with a numerical aperture of 0.5 NA, a pinhole size of 84 μm, a step size of 1 μm, a PMT gain of 1107 V, an offset of 2.7%, and a laser intensity of 67%. A minimum of three intensity curves were averaged for each inhibitor molecule concentration and normalized to the maximum intensities. These concentration-dependent intensities were fitted with a modification from the generalized logistic function we implemented in Origin software (OriginLab) using a Levenberg-Marquardt algorithm with a tolerance of 10^{-9} and maximum number of 400 iterations. The resulting fitting curve is plotted along with the 95 % confidence intervals as well as the 95 % of prediction intervals. The fitting procedure delivers the half-maximal inhibitory concentration (IC_{50}) needed to replace the dye.

2.2 Quantum Mechanical Simulations

The density functional theory (DFT) calculations for the parametrization of the force field were performed with the Vienna Ab initio Simulation Package (VASP), version 5.44.[35,36] The Perdew, Burke and Ernzerhof (PBE) generalized-gradient-approximation exchange-correlation functional was used,[37] describing the valence-electron/ion-core interactions by projector augmented-wave (PAW) potentials. The cutoff value was set at 450 eV. Convergence criteria of 10^{-6} eV and 0.02 eV Å^{-1} were used for total energies and forces, respectively. In all surface calculations a $3 \times 3 \times 1$ k-point sampling was employed. Dispersion interactions were included via the Grimme D3 empirical vdW correction.[38] Selected systems were computed also with the Grimme's D2 empirical correction,[39] including a variant in which the C6 parameters of Zn have been replaced with the previous noble gas,[40] and the Tkatchenko-Scheffler[41] (TS) dispersion correction, for comparison. The slab model of the $(10\bar{1}0)$ surface was generated by carving out of the optimized bulk structure[42,43] a (4×2) super cell with dimensions of (13.15×10.60) Å^2 in the periodically repeated (x, y) plane. In the z direction, the cell parameter was set to 24.79 Å to keep the slab separated from its periodic images by 15 Å. The OH-terminated surface model was extracted from the DFT-based molecular dynamics calculations of Meyer et al.,[44] which identified an equilibrium between dissociatively and molecularly adsorbed water molecules, and geometrically optimized.

To check for the protonation state of the amino acids in methanol, metadynamics simulations were performed with DFT simulations with the CP2K code.[45] The Quickstep technique with a mixed plane wave and Gaussian basis set methodology (Gaussian and Plane Wave method, GPW) was employed to calculate the electronic structure. We used the PBE functional,[37] with the Goedecker–Teter–Hutter pseudopotentials and a triple-zeta basis set with polarization functions (TZVP) augmented with the empirical Grimme's D3 correction.[38] The cutoff of the finest grid level, for the plane wave basis, was set to 400 Ry. A proton was transferred from the backbone amine group to the backbone carboxyl group of glycine, solvated in both water and methanol. A single glycine molecule was put in the middle of

a 12 Å cubic box, filled with solvent molecules. Well-tempered metadynamics simulations were run, after a brief system thermalization, for 50 ps at 300 K in the NVT ensemble using the neutral Sampling through Velocity Rescaling (CSVR) thermostat,[46] with a time step of 0.5 fs. The chosen collective variable, describing the proton transfer, was d=d_{NH}-d_{OH}, i.e. the difference between the distance of the proton from the nitrogen and from one oxygen of the carboxyl group. Hills were added every 20 steps, with initial height $6{\cdot}10^{-3}$ Ha, a width of 0.2 bohr, and a well-tempered γ of 50.

Additional DFT simulations, both static and dynamic, on selected configurations were performed with the CP2K code, at the same PBE-D3 level of theory.

2.3 ZnO force field parametrization

Parameters for the ZnO surface and its hydroxyl termination were developed to be compatible with the TIP3P water model and the Charmm36m force field[47] employed for the amino acids. This means that the standard Lorentz-Berthelot combination rules can be employed to determine the pair-wise Coulomb and Lennard-Jones (LJ) interactions. Energy-distance curves were recorded with both DFT and force field energy calculations and compared (Figures S2-S7 in Supporting Information). The reference-test molecules consisted of: water, methanol, glycine, imidazole (representative as the side chain of histidine) and methanethiol (representative as the side chain of cysteine). Starting from a fully minimized configuration, each molecule was displaced vertically along the surface normal, and total energy calculations were performed at each separation, keeping all atomic positions fixed. The reference calculations were performed using the DFT approach detailed in the previous section. The classical energies were computed using the GULP simulation package.[48] Both the DFT and the classical energy values were rigidly shifted to obtain a value of 0.0 eV for a molecule-surface separation of 6 Å. A detailed view of the employed parametrization can be found in the Supporting Information (Figure S1). Briefly, the point charges of zinc and oxygen atoms of the ZnO slab model were set to the values of +1.2 e and -1.2 e respectively. The

choice of the optimal LJ parameters for ZnO was based on the best agreement between DFT and classical energy landscapes. For the surface termination, charges of Os and Hs attached to the surface were set to values close to the free TIP3P water molecule (-0.834 e and +0.417 e, respectively). Following the same reasoning, also their LJ parameters were set to their TIP3P values. Additional bond and angle terms were defined for the Zn-O-H and O(Zn)-H groups, while the rest of the ZnO surface was kept fixed during the simulations. Two parameter sets were considered, one employing combination rules for all atom pairs and one in which the peculiar N-Zn pair interaction was defined by explicit LJ parameters (and not computed via the usual combination rules).

2.4 Classical Molecular Dynamics (MD) simulations

Simulations were performed with Gromacs 2019[49] employing the Charmm36m force field[47] for the amino acids, in combination with the above defined ZnO parameters. For the solvents, we employed the Charmm-modified TIP3P water model and the Charmm generalized force field (CGenFF)[50] parameters for methanol, as implemented in Fischer et al..[51]

The employed ZnO surface slab was generated starting from a 2×2 super-cell of the DFT model, resulting in an area on the xy plane of $(26.30 \times 21.20)\,\text{Å}^2$. The surface slab was separated from its periodically repeated image along the z coordinate by about 40 Å resulting in a free volume above the surface which was filled with solvent molecules. Most of the simulations in methanol were run on a surface sporting a 25% water monolayer dissociation. Additional simulations were run on a bare ZnO surface and a surface with 50% water monolayer dissociation. For the reference structure in water, based on the DFT molecular dynamics calculations of Meyer et al.,[44] only a 50% water monolayer monolayer dissociation was considered. For every dissociated water molecule, an OH group was put on top of a surface Zn atom and the remaining proton was put on a neighboring surface O atom. Considering the OH groups, the 25 and 50% cases correspond to a surface density of 1.44 and 2.87 OH/nm^2, respectively.

Solvent molecules were put in the simulation boxes to fill the volume. Different amounts were probed, after 10 ns NVT equilibrations, to check whether the TIP3P and methanol standard bulk densities were reached in the middle of the cell. This resulted in 693 water molecules and 335, 325 and 315 methanol molecules for the 0%, 25% and 50% dissociation cases, respectively.

Bonds involving hydrogen atoms were constrained by means of the LINCS algorithm.[52] The Particle Mesh Ewald (PME) method was used for the calculation of the electrostatic interactions, using a cut-off distance of 1.0 nm for the real-space part of the Ewald sums and the van der Waals interactions. All surface atoms except the dissociated waters were kept fixed in their equilibrium positions. Prior to the production runs, the systems were equilibrated in a series of energy minimizations and NVT runs for about 1 ns, according to standard protocols. Constant-temperature simulations were performed in an NVT ensemble with a modified Berendsen thermostat with a coupling constant of 0.1 ps.[46] A Verlet integration time step of 2 fs was used. Visualization and analysis of the trajectories were performed with VMD.[53]

2.5 Free energy calculations

The free-energy landscapes were computed by adding an adaptive bias potential during the course of the MD runs according to the metadynamics scheme in the well-tempered ensemble (wt-MetaD),[54] as implemented in the PLUMED 2.5 package.[55,56] As a collective variable (CV) we chose the height h of the center of mass of the amino acid molecule with respect to the surface. Gaussian hills with an initial height of 0.24 kcal mol^{-1} and a full width at half maximum of 0.3 Å were added every 0.6 ps. The bias factor was set to 20 and the grid spacing to 0.1 Å. A potential wall was set 15 Å above the surface to limit the interaction to only one face of the ZnO slab.

To enhance the sampling of the simulations, metadynamics was coupled with Replica Exchange with Solute Tempering (REST).[57–59] A selected part of the system was defined as

the 'solute' in the REST simulations, whose temperature was scaled in the different system replicas ('hot' system region). In our final implementation (cf. Results and Discussion) the solute comprised both the amino acid and the ZnO surface, in order to disrupt the surface-solvent interactions. The rest of the system remained at the base temperature $T_0 = 300\,K$ ('cold' system region). We used 8 replicas at temperatures T_i corresponding to 300, 322.711, 347.142, 373.421, 401.691, 432.1, 464.812, and 500 K, respectively. Exchanges between the replicas were attempted every 400 fs, following a Metropolis-Hastings acceptance criterion. The geometric progression of the temperatures T_i ensured a nearly uniform overlap of the potential energy distributions and thus a uniform acceptance probability across the replica ladder, with average values $> 30\,\%$ in the simulated systems. The round-trip time, which is defined as the time needed by one replica to move along the complete temperature ladder from 300 to 500 K and back, amounted to around 1.2 ns, with minimal variations among the simulated systems.

3 Results and Discussion

We recently introduced a platform for screening abiotic/biotic interactions based on an optically sectioned indicator displacement assay (O-IDA).[33] In this platform, a fluorescence dye (indicator) with a specific affinity for the coordinated zinc atoms on the single-crystalline ZnO surface is displaced by the amino acids depending on their concentration and own binding affinity. This leads to a dose-response curve, from which the half-maximal inhibitory concentration IC_{50} can be estimated. The latter is related to the inhibitory binding constant K_i, which allows for the calculation of binding free energies. In our previous studies we selected the amino acids histidine (His) and cysteine (Cys), because on their presence in zinc finger proteins,[60] and serine (Ser) as a known binding partner within ZnO-binding peptides.[61] In addition to these three amino acids, for this study we included also tryptophan (Trp), in order to investigate the adsorption of an amino acid with a bulky aromatic functional

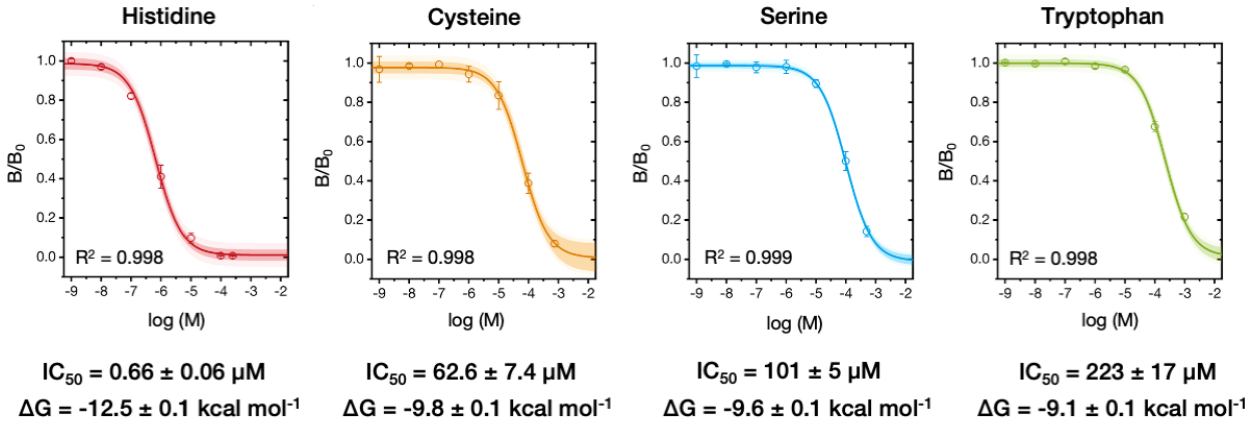

Figure 1: *Binding affinities of four amino acids on the $(10\bar{1}0)$ ZnO surface in methanol determined by O-IDA.*

group. Fig. 1 reports the dose response curves for the four amino acids and their binding free energies to the $(10\bar{1}0)$ ZnO surface in a methanol environment. While we can obtain reliable information regarding the binding affinities from this assay, we need computational approaches to discover the atomistic details of the underlying interactions.

Following the path laid down in the Introduction, we computationally reproduced these experimental binding energies by facing and overcoming the four challenges there listed and the results are presented here accordingly.

3.1 A classical potential for ZnO/solvent/biomolecules interfaces

We propose here a simple parametrization for the interactions between the reconstructed ZnO $(10\bar{1}0)$ and solvated biomolecules. For the purpose of this work, the atoms within the ZnO crystals were constrained to their equilibrium positions, which is a common approximation when considering surface adsorption of soft matter or small organic molecules. Therefore, only non-bonded interactions between the Zn and O atoms and the solution environment (including the biomolecules) needed to be parametrized. In the process we were guided by the following requirements: 1) simplicity, i.e. as few as possible atom types and parameters, to increase transferability; 2) compatibility with the most common biomolecular force fields,

i.e. the standard Lorentz-Berthelot combination rules can be employed to determine the pair-wise interactions; 3) consideration of a properly terminated surface, to mimic realistic conditions; 4) validity in both aqueous and organic (methanol) solutions. As far as we know, only one parameter set for ZnO has been proposed in the literature[27,62] fulfilling the first two requirements. However, it lacked a realistic representation of the surface/solvent interface and validation against experimental observables.

The parametrization procedure we followed is quite standard and is described in the Materials and Methods. As a reference surface, we opted to employ the ZnO $(10\bar{1}0)$ surface terminated by water, sporting the previously described (2×1) superstructure, caused by the dissociation of every second water molecule in the first solvent monolayer.

We described the interactions of the surface with adsorbates by a Lennard-Jones and Coulomb non-bonded potential. We identified 4 atom types on the surface: surface Zn, surface O, and the O and H of the hydroxyl functionalities. Bader charges for the first two types, computed at the DFT level, resulted in a value of about $\pm$ 1.6 e. However, these charges are not guaranteed to reproduce well the electrostatic interactions between the oxide layer and the adsorbed species. Indeed, most common force fields for water or biomolecules use point charges best fit to reproduce the electrostatic potential felt by interacting species (ESP charges). We thus computed ESP charges for the Zn and O atoms of the first material layer, which were $\pm$ 1.2 e. Regarding the hydroxyls, we opted to employ the TIP3P point charges, given the origin of these functionalities from dissociated water.

This left the four LJ parameters for the surface atoms to be determined. We determined these parameters from a fit of the energy landscape of a test set of molecules desorbing from the surface. Also in this case, the best agreement was obtained when setting the hydroxyls' LJ parameters to the Charmm modified TIP3P values.

Figure S2-7 in Supporting Information reports all the tested energy curves, while Fig. 2 report four exemplary cases. For all systems, we computed the DFT curves with and without the inclusion of dispersion interactions, as described by Grimme's D3 correction with

Becke-Jonson dumping.[38] In all cases the inclusion of dispersion causes severe shifts in the depth of the attractive potential wells, while mostly retaining the equilibrium distance position. The effect is particularly relevant for the Zn-N interaction in imidazole where the binding energy shifts by about 10 kcal mol^{-1}. The chemical bonding in ZnO is predominantly covalent but with a significant contribution from ionic bonding. To make sure we did not overestimate the vdW attraction, due to the D3 parameterization of Zn, for selected cases, we also computed the energy curves with the Grimme's D2 empirical correction,[39] including a variant in which the C6 parameters of Zn have been replaced with the previous noble gas,[40] and the Tkatchenko-Scheffler dispersion correction.[41] All dispersion-including curves basically overlay with each other, with the expected differences resulting from the known drawbacks and strengths of each method.[40] Based on these results we then decided to fit our LJ parameters to the D3 curves.

As can be seen in Fig. 2, in all cases a very good agreement between the final parameter set and the DFT curves was obtained. Some minor deviations were observed for the repulsive curves but overall the force field reproduced the repulsion quite well. Slightly better agreement was observed for the interactions with the Zn atoms than with the O atoms of the surface, but deviations were always within a few kcal mol^{-1}. Importantly, the relative simple definition of the parameter set is able to reproduce the shape of the curves in all diverse situations. Following the requirements we set for our parameterization, the force field is able to reproduce interaction curves for both water and methanol, allowing us to simulate the system in both solvent environment.

One notable exception in the agreement is the Zn-N interaction in the imidazole case (Fig. 2b). The interaction between histidine (i.e. imidazole) and zinc ions is known from analogous biological systems (zinc-finger proteins)[60,63] to be highly specific and has been studied with DFT simulations.[64,65] The curve obtained with the simplest definition of the force field, in which the pair interaction is defined only by the general individual charges and LJ parameters via combination rules, is in between the pure DFT curve and curves based

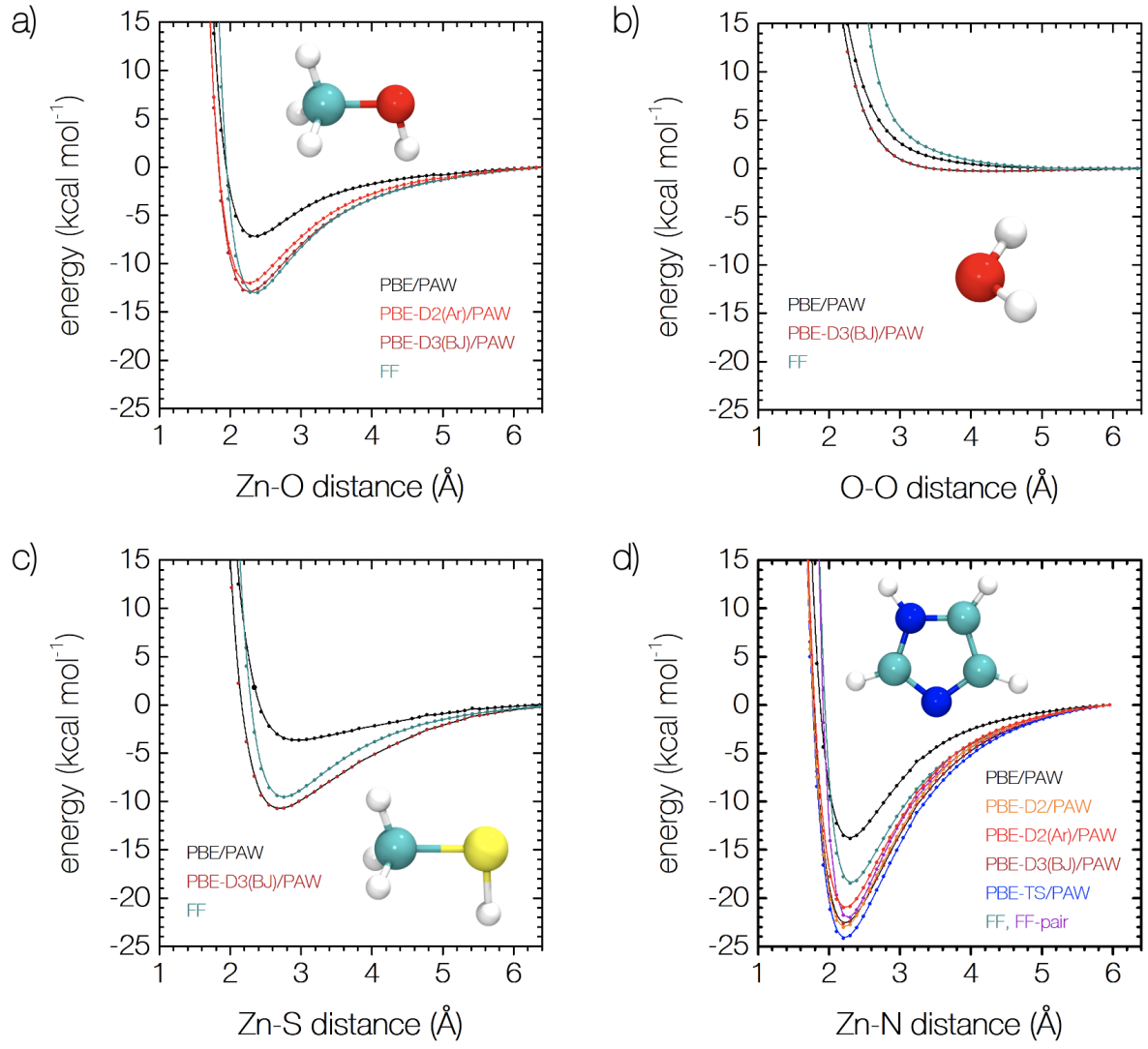

Figure 2: *Distance-energy curves for a) methanol (Zn-OH interaction), b) water (O-O repulsion), c) methanethiol (Zn-S interaction), d) imidazole (Zn-N interaction). Both DFT and classical (FF) curves are provided. In the case of DFT, a comparison between calculations without (PBE/PAW) and with dispersion corrections is provided. Considered corrections, for selected cases, are Grimme's D2 empirical correction (PBE-D2/PAW), including a variant in which the C6 parameters of Zn have been replaced with the previous noble gas (PBE-D2(Ar)/PAW), Grimme's D3 empirical vdW correction (PBE-D3(BJ)/PAW) and Tkatchenko-Scheffler (PBE-TS/PAW) dispersion correction.* In d) also the force field variant with explicit Zn-N pair parameters is reported (FF-pair). Curves are accompanied by ball and stick representations of the investigated molecules (Color code: O, red; C, cyan; N, blue; S, yellow; H, white). Additional distance-energy curves are in Supporting Information (Figures S2-7).

on dispersion corrections. Since this interaction is crucial to the adsorption of histidine on the surface, we devised an alternative version of the force field (FF-pair in Fig. 2b) in which specific pair LJ parameters are included to describe the N-Zn interaction, resulting in an overlay with the D3 curves.

3.2 Effect of the solvent on the physical and chemical surface features

Understanding surface properties and surface termination is essential for the atomistic understanding of the binding behavior as well as comparison between experimental approaches and simulations. The specific recognition of materials by small biomolecules is often mediated by the sensing of the local changes in the solvent density at the solid/liquid interface at the molecular level.[25,66]

While the surface termination of the the ZnO $(10\bar{1}0)$ surface in aqueous conditions has been extensively studied,[42,44,62,67] the surface termination in MeOH under experimentally relevant conditions is unknown. Both experiments and simulation studies in aqueous conditions revealed that a dynamic equilibrium exists between the half and the full dissociated monolayer of water molecules. Switching between these two states occurs via a dynamical process of proton association and dissociation.[67]

Only a few studies have investigated the interface between specific ZnO surfaces[68,69] and methanol and mostly assumed a contact between a pristine ZnO surface and methanol. However, the single-crystalline substrates used in our work were synthesized in an aqueous environment, stored under ambient conditions and cleaned with an UV-Ozone treatment before being placed in contact with methanol. Comparing the most stable predicted $(10\bar{1}0)$ surface terminations in water and methanol at low coverage,[44,68] the same superstructures are obtained for an adsorbed monolayer, with different surface groups depending on the environment. However, a stronger binding energy per molecule is found for H_2O. Under the assumption that the accessible binding sites are occupied with molecularly adsorbed

and dissociated water molecules forming a half-dissociated (2×1) structure, it is uncertain whether replacement of the water solvent with methanol would lead to a full exchange of the surface groups.

To address the question of the surface protonation four different terminations have been considered for the methanol environment: a bare surface; two surfaces hydroxylated by a 25% or 50% dissociation of an adsorbed water monolayer, respectively, upon removal of the molecularly adsorbed water molecules; a surface reconstructed by a 50% dissociation of an adsorbed methanol monolayer, resulting in a distribution of buried OHs and exposed methoxy functionalities, according to the superstructures described from Kiss et al.[68] (Figure S8 in Supporting Information).

To assess the role of different solvents in the investigated system, we filled the simulation box over each of the surface models with either water or methanol. Fig. 3 reports the mass density profiles for the two solvents at the ZnO interface. For methanol, the surface after a 25 % water monolayer dissociation is chosen for this figure. A clear structuring induced by the surface was observed, with peaks and minima corresponding to the various solvation layers. As is common for solvent/oxide interfaces, the water density in the interface regions displays evident oscillations that level out and reach the expected bulk density values. Interestingly, a much stronger solvent structuring can be observed in the case of methanol, with bulk density achieved only at over 15 Å from the surface together with a large depletion zone at about 5 Å from the surface. This solvent structuring is expected to strongly impact the adsorption behavior of the amino acids.

A first validation of the developed potential parameters is performed by comparing the value of the heat of immersion of our investigated ZnO surfaces predicted by our potential with available experimental data. The heat of immersion (E_{im}) is defined as the enthalpy gain per unit surface area (A) resulting from placing a dry surface in contact with water or methanol, respectively. It can be computed classically from the potential energy difference between a slab surface model in contact with bulk solvent ($E_{interface}$), the same slab model

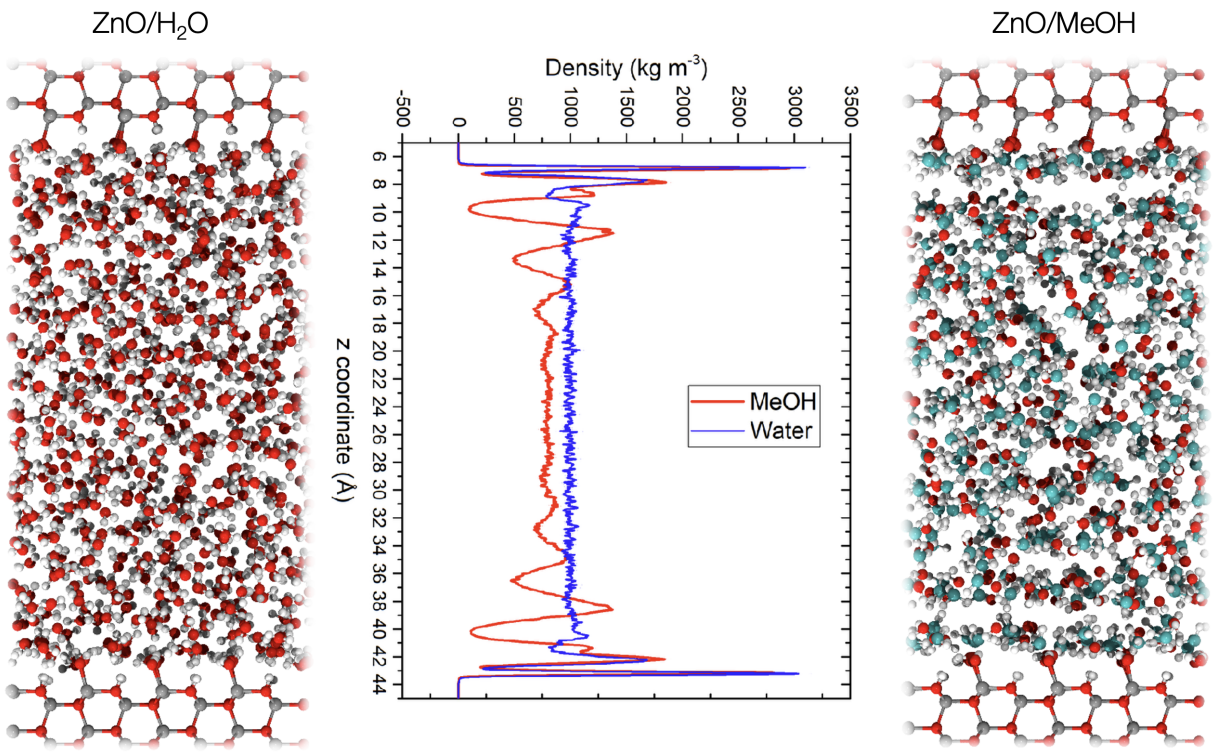

Figure 3: *ZnO/solvent interaction. Middle: mass density profiles for water and methanol at the ZnO interface. Due to periodic boundary conditions the profiles are symmetric, with interactions on both faces of the slab. Left and right: visualization of the equilibrated ZnO/water and ZnO/methanol models, respectively. Color code: Zn, grey; O, red; C, cyan; H, white.*

in vacuum ($E_{surface}$) and a bulk solvent cell with the same number of solvent molecules as included in the interface model ($E_{solvent}$), all obtained as averages along MD simulations at constant temperature (300 K) and pressure:

$$E_{im} = \frac{E_{surface} + E_{solvent} - E_{interface}}{2A} \quad (1)$$

The value for the heat of immersion in an aqueous environment calculated from Eq. 1 for our surface model is 0.60 J m^{-2}, which is in the lower range of the reported experimental values from 0.4 to 1.4 J m^{-2}.[70,71]

For our four different surface models considered in methanol, we find 0.46 J m^{-2} for the 50% dissociated methanol monolayer, 0.57 J m^{-2} for the 50% dissociated water monolayer, 0.65 J m^{-2} for the 25% dissociated water monolayer and 0.71 J m^{-2} for the bare surface. The

experimental value for E_{im} for ZnO in methanol is reported as $0.80 \pm 0.17\,J\,m^{-2}$.[71] Our calculated values for the 25% dissociated water monolayer and the bare surface are within this range. Particularly, the result obtained for the 50% dissociated methanol monolayer suggests that this termination is not compatible with the corresponding experimental values, consolidating the hypothesis that an amount of OH group terminate the $ZnO(10\bar{1}0)$ surface under common experimental conditions. Our hypothesis is that a complete water/methanol termination replacement is not likely, and that an amount of OH groups remain bound to the surface. To support this, we have performed a short ab initio MD simulation of a methanol monolayer interacting with the $ZnO(10\bar{1}0)$ surface presenting a 25% coverage of dissociated water. While some proton-exchange dynamics was observed between the adsorbed methanol molecules, the ZnO atoms and the hydroxyl groups, we neither observed any spontaneous methanol dissociation, nor any OH recombination and desorption of molecular water during 2 ps of simulation time. While these results indicate a smaller coverage of hydroxyl groups in comparison with the aqueous environment, the results are not conclusive and further tests will be carried out in section 4, where the free energy of adsorption is investigated for one amino acid (His) on the four surface models in the methanol environment. However, the protonation state of amino acids in methanol need to be investigated first.

3.3 Protonation state of amino acids in non-aqueous solvents

It is known that the canonical form of glycine is stable in the gas phase, while the zwitterionic form is stable in the solid phase or in aqueous solution. This dependency on the surrounding environment is due to a stabilization of the zwitterion through H-bond formation. The canonical-to-zwitterionic transition has been extensively studied by DFT, obtaining results in agreement with experimental findings.[72,73] On the other hand, information on the protonation state of amino acids in non aqueous solvents is scarce, with no data available, to the best of our knowledge, for pure methanol solutions as employed in our O-IDA measurements. However, this information is crucial for classical simulations, where the protonation state of

the biomolecule has to be set *a priori*, and is expected to have a significant impact on the adsorption behavior.

To identify the preferential protonation form for amino acids in methanol, the interconversion between the zwitterionic and canonical form of glycine was followed using DFT well-tempered metadynamics and compared with an aqueous environment. The intention was not to aim for exact values of the free energy difference, but to get a qualitative overview of the relative stabilities in the two solvents. Interestingly, during equilibration, starting from canonical glycine in water and methanol, in both cases the amino acid spontaneously transformed into the zwitterionic form very quickly, remaining in this configuration until the end of the equilibration (Figure S9 in Supporting Information). After a short equilibration, a single collective variable was chosen to explore the free energy surface, namely the transition of a hydrogen from the terminal amino group to the terminal carboxyl group (cf. Materials and Methods for the details). The two free energy profiles obtained for water and methanol are displayed in Fig. 4.

As expected, the zwitterionic form is significantly more stable than the canonical one in water. Interestingly, the same is valid also for methanol, although the free energy difference between the two forms is lower than the aqueous case. This can be explained with the polarity index of methanol, which is reduced by almost half in comparison with water. However, the free energy difference between the two states is still so large that we expect zwitterionic glycine to be the dominant species in pure methanol solution.

These results also suggest that the other amino acids should be mostly zwitterionic in methanol. Nonetheless, since our results for glycine cannot straightforwardly be transferred to the other molecules, we still investigated both the zwitterionic and canonical forms of all amino acids, and compared their computed binding free energy on ZnO in methanol with the experimental measurements. For histidine, that can have different protonation states in the side chain, we focused on its canonical form with the δ-nitrogen protonated (Hid).

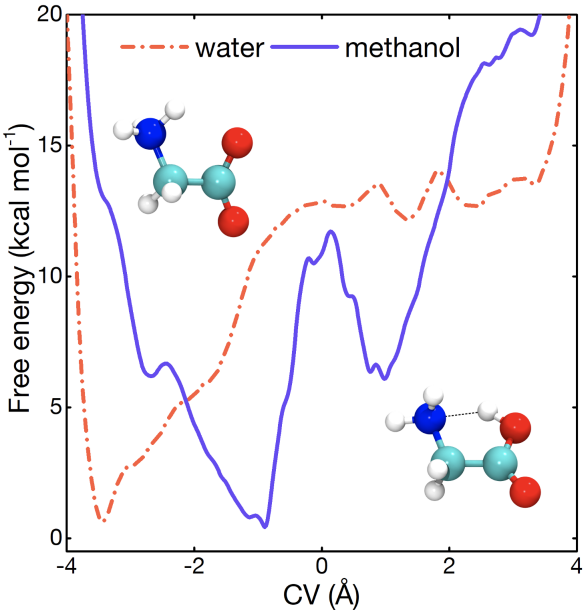

Figure 4: *DFT wt-MetaD free-energy profiles computed for the transition of a proton from the terminal amino group to the terminal carboxyl group of glycine in methanol (solid purple line) and water (orange dot-dashed line). The zero of the free energies is set at their minimum value. The zwitterionic and canonical forms of glycine are reported in correspondence of the CV regions in which they exist.*

3.4 Accurate quantification of binding free energies using enhanced sampling methods

The accurate measurement of the free energy of adsorption of the selected amino acids on ZnO($10\bar{1}0$) in methanol were used as the proving ground for our computational approach. Assuming that we are able to calculate a converged free energy profile $G(h)$ with respect to the height h of the amino acid's center of mass with respect to the surface, the free energy of adsorption ΔG_{ads} can be computed as

$$\Delta G_{\mathrm{ads}} = -k_{\mathrm{B}} T \ln \left(\frac{\rho_{\mathrm{ads}}}{\rho_{\mathrm{dis}}} \right) , \tag{2}$$

where k_B is the Boltzmann constant and T the temperature of the system. ρ_{ads} and ρ_{dis} are the probabilities of finding the amino acid in an adsorbed or in a dissolved state, respectively,

which can be computed by Boltzmann integration of $G(h)$:

$$\rho_{\text{ads}} = \frac{1}{h_0 - h_{min}} \int_{h_{min}}^{h_0} \mathrm{e}^{-\beta G(h)} \mathrm{d}h \ , \tag{3}$$

$$\rho_{\text{dis}} = \frac{1}{h_{max} - h_0} \int_{h_0}^{h_{max}} \mathrm{e}^{-\beta G(h)} \mathrm{d}h \ . \tag{4}$$

The boundaries of the integrals define the regions in which the molecule is either in the adsorbed ($h_{min} < h < h_0$) or the dissolved state ($h_0 < h < h_{max}$). The lower limit h_{min} is usually the position at which $G(h_{min}) = 0$ and the upper limit h_{max} is the largest set value of the variable h in the enhanced-sampling simulation employed to compute $G(h)$. The choice of h_0 is arbitrary, but can be set as the lowest h value for which the $G(h)$ profile becomes flat after reasonable convergence of the MetaD trajectory, indicating that the amino acid does not experience any surface interaction and behaves as in bulk solution. Small variations of the set h_0 value do not affect ΔG_{ads} at all, as long as the profile presents a clear energy minimum in the adsorbed state.

Our method of choice to obtain the required free energy profiles for the four considered amino acids was well tempered metadynamics (wt-MetaD), as detailed in the Materials and Methods. The feasibility of this method for the evaluation of biomolecule/oxide interactions has been proven by some of us for the case of peptide adsorption on titania[25] and silica.[74] The convergence of wt-MetaD alone can be hindered when other important slow degrees of freedom, apart from the biased collective variable, are neglected. This is particularly true for biomolecules, such as polypeptides, that possess a remarkable conformational freedom. For this reason, in previous works, wt-MetaD has been augmented by Replica Exchange with Solute Tempering (REST).[57–59] In the REST method, the bonded and non-bonded interactions of a selected part of the system (the 'solute') are heated up in multiple system replicas, to enhance the system sampling and the simulation convergence.

While the REST-sampling of intermolecular degrees of freedom could be neglected when

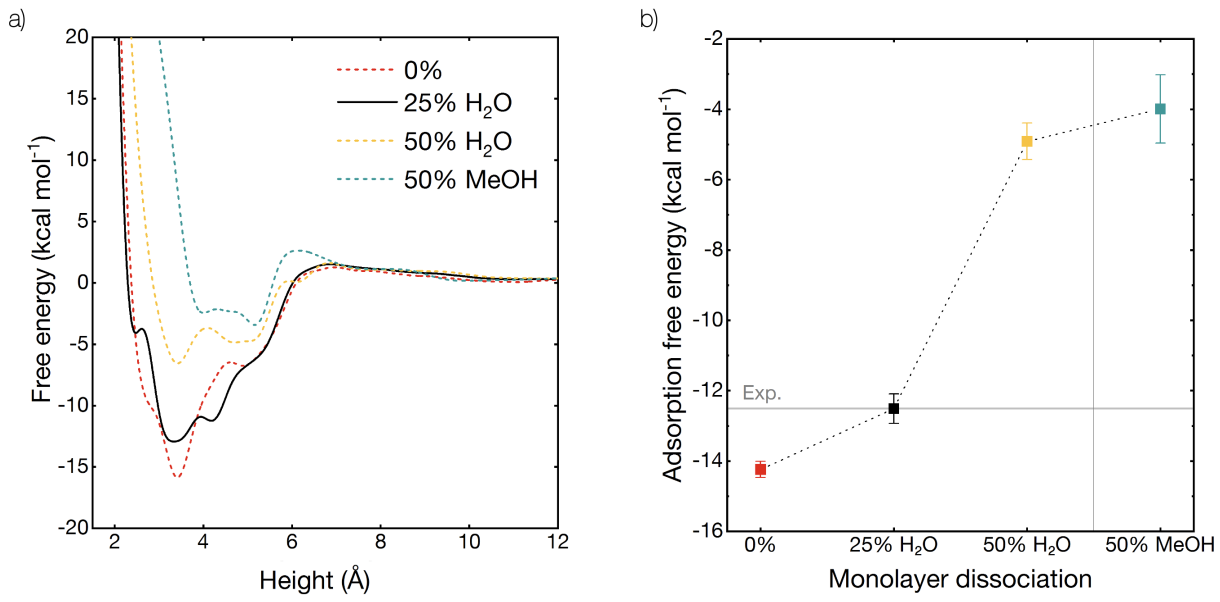

Figure 5: *a) Converged free energy profiles computed for zwitterionic Hid adsorption in methanol on the ZnO (10$\bar{1}$0) surface, for the cases: 0%, bare surface; 25%, hydroxylated by a 25% dissociation of an adsorbed water monolayer; 50%, hydroxylated by a 50% dissociation of an adsorbed water monolayer; reconstructed by a 50% dissociation of an adsorbed methanol monolayer. The zero of the free energies is set at the minimum value in the solvent bulk phase. b) Hid adsorption free energy, computed as in Eq. 2, as a function of the dissociation of an adsorbed solvent monolayer. Grey line: O-IDA binding free energy.*

considering the simpler case of amino acid adsorption, attempts to converge $G(h)$ for our systems in water or methanol with pure wt-MetaD failed (cf. Figure S11 in Supporting Information). This was due to a deficient sampling of the area in proximity to the surface (cf. Figure S10 in Supporting Information). Indeed, wt-MetaD has been shown to very poorly converge in the case of molecules interacting with material surfaces with high solvent affinity, due to the inherent difficulty of displacing water molecules within the strongly adsorbed solvent layer.[30] This is true also for the ZnO (10$\bar{1}$0) surface, where the distinct solvent rearrangements induced by the surface (Fig. 3) can create entropic barriers to the adsorption process. We would like to note that this is not necessarily due to a high free-energy barrier along the $G(h)$ profile, but to the narrowness of the adsorption pathway that can lead to successful displacement of the chemisorbed water layer by the amino acids. Solvent interference in the computational prediction of ligand binding in protein pockets is a known

issue that has been partly overcome by extensions of the wt-MetaD approach. In particular by funnel metadynamics[32] and Sampling Water Interfaces through a Scaled Hamiltonians (SWISH) algorithm by Comitani et al.,[31] in which the pocket/water interactions are re-scaled in a replica exchange approach.

In fact, coupling our wt-MetaD simulations to a REST approach, in which the amino acids were treated as the 'solute', already significantly improved the sampling of the CV space close to the surface (cf. Figure S10 in Supporting Information). However, this approach still failed in converging the adsorption free energies towards a value close to the experimental data (cf. Figure S11 in Supporting Information). Only after the ZnO surface atoms were also considered as 'solute' (i.e. after re-scaling the ZnO/solvent interactions, which is similar in essence to the SWISH approach), were we able to achieve a good convergence of the ΔG_{ads} values within a reasonable simulation time.

The results obtained for the adsorption of the zwitterionic form of histidine (Hid protonation state), from bulk methanol to the four ZnO $(10\bar{1}0)$ surface terminations described in Section 2 are presented in Fig. 5. The free energy profiles (Fig. 5a), plotted against the height of the center of mass of the amino acid with respect to the surface, are well converged after 1000 ns of simulation (see Fig. 6a for the 25% case), with the final shape and relative minima position already appearing before 500 ns. On all hydroxilated surfaces, the global minimum is in close proximity to ZnO, showing that the amino acid favors the adsorbed state with respect to solution, as predicted by the experiment. For the surface after 50% methanol monolayer dissociation, the global minimum is farther from the surface, due to steric hindrance by the methoxy functionalities. No appreciable free energy barrier is observed between the two states. This confirms that the previously observed sampling issues were indeed not due to a high activation barrier to be crossed in order to approach the surface, but to the narrow channel connecting the two states, most probably dependent on the reorganization of the ordered first solvation layer.

Interestingly, the position of the global minimum is the same in all cases, apart the 50%

methanol monolayer dissociation one, at about 3.5 Å from the surface, suggesting that the main mode of interaction with ZnO is independent of the amount of surface hydroxylation. However, the depth of this free energy well together with the shape and relative stability of other local minima close to the surface, shows a strong variability with respect to surface hydroxylation. A local minimum closer to the surface, at about 2.5 Å, for example, is absent in the 0% water dissociation case, suggesting that this configuration is not reachable for highly hydroxylated surfaces.

The computation of ΔG_{ads} via Eq. 2, averaged along the final 300 ns of simulation, confirms the strong impact of surface termination on the interaction (Fig. 5b). Unsurprisingly, the bare surface is able to attract more strongly the amino acid, with an adsorption free energy of -14.2±0.2 kcal mol^{-1}. In the intermediate hydroxylated case (25%), the strength of adsorption is slightly decreased (-12.5±0.4 kcal mol^{-1}), while the 50% surface sees a dramatic reduction in binding free energy, down to -4.9±0.5 kcal mol^{-1}. The adsorption free energy further decreases in the case of the surface reconstructed by a 50% dissociation of an adsorbed methanol monolayer, due to both the bulkiness and the apolarity of the methoxy functionalities that decorate the surface in this situation. Remarkably, the experimentally measured adsorption free energy for histidine in methanol on the ZnO $(10\bar{1}0)$ surface (Fig. 1) almost exactly matches the computed value in the 25% case. This agreement is a first validation of our entire simulation approach, from the potential parametrization up to the applied enhanced-sampling algorithm.

Together with the predicted heat of immersion reported beforehand, these results motivated us to focus our subsequent investigation on the ZnO $(10\bar{1}0)$ surface with an OH coverage of 25% with respect to a dissociated monolayer of water.

Fig. 6 reports the free energy profiles $G(h)$ for the four investigated amino acids, in their zwitterionic form. The convergence of $G(h)$ is very good in all cases. All four molecules are predicted to spontaneously adsorb on the ZnO surface from bulk methanol. The shape of the profiles in proximity to the surface is considerably different among the amino acids,

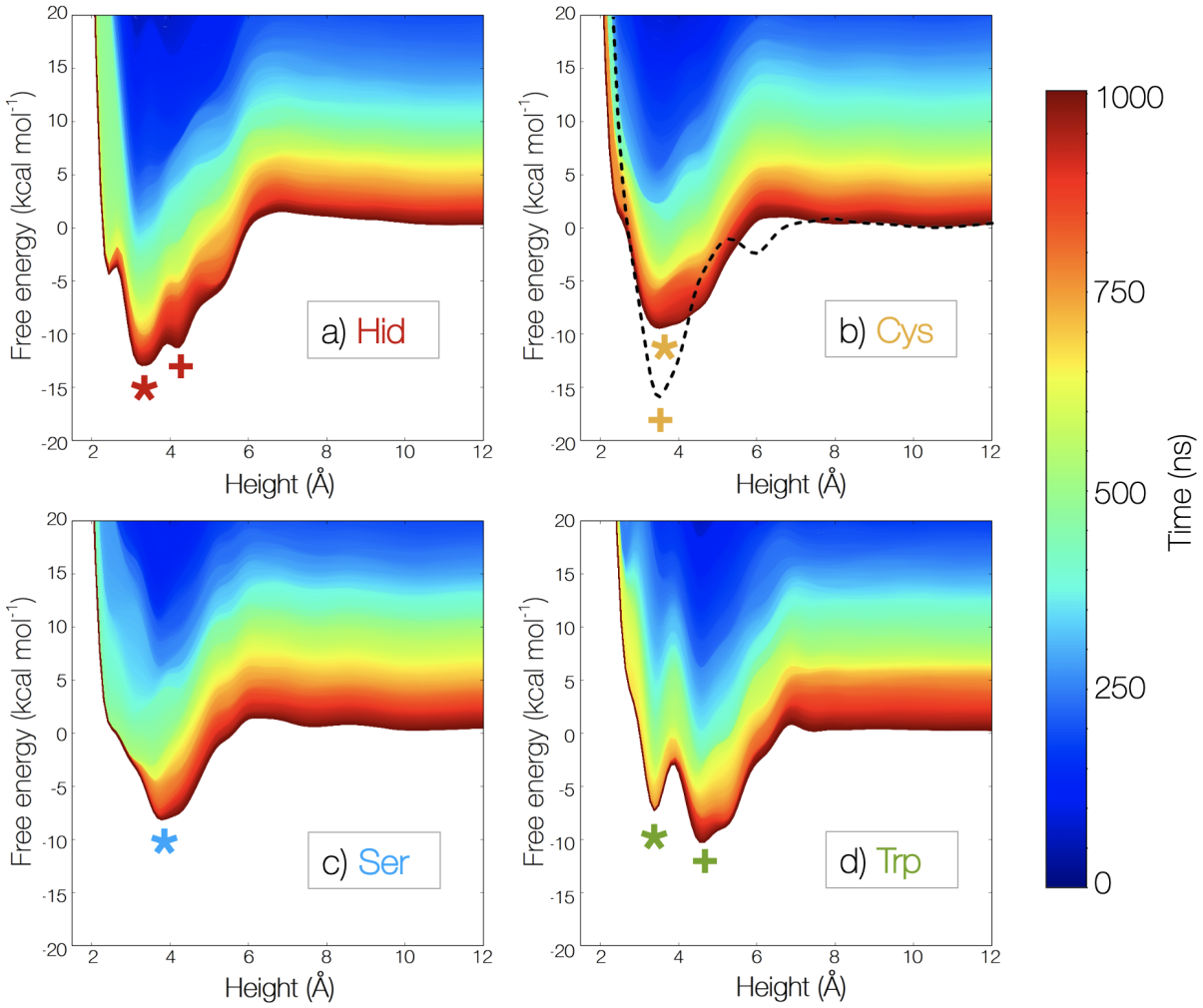

Figure 6: *Free energy profiles for the zwitterionic forms of Hid (a), Cys (b), Ser (c) and Trp (d) adsorption in methanol on the ZnO (10$\bar{1}$0) surface. The evolution of the profiles during the REST-MetaD simulations is reported, according to the color scale on the right. The zero of the free energies is set at the minimum value in the solvent bulk phase. In b), the dashed line reports the free energy profile for Cyn. The * and + markings identify the minima, from which the configurations are extracted in Fig. 8 and Fig. 9*

suggesting different modes of interaction with the surface. His and Trp show multiple adsorption minima, while a broader individual global minimum is computed for Cys and Ser, probably due to their smaller size. For Cys, Ser, and His, no free energy barrier separated the adsorbed and dissolved states, while a small one was observed for the Trp case, possibly a result of its increased apolarity.

Evaluating metadynamics convergence by looking at the shape evolution of the free energy profiles can be prone to errors. A better approach is to evaluate the temporal evolution of an observable, such as ΔG_{ads} (Fig. 7a)). Abrupt changes in the computed values can be observed well up to 400 ns of simulation, with the values still prone to change even later in the calculation. After 600 ns, most adsorption free energies are oscillating around a final value, with Ser still showing a slow increase and Trp showing some oscillations. This is due to the fact that the ergodicity of the sampling is not fully guaranteed, not even under the strong bias provided by the combination of replica exchange with metadynamics. In fact, although all investigated systems explore the whole ranges of the phase space well enough, the sampling of single replicas is not always ideally homogeneous (diffusive).[75] This behavior, however, is much improved with respect to standard wt-MetaD and simple REST-MetaD (Figures S11 in Supporting Information), where no convergence could be assumed even at very long simulation times. Because of these residual convergence issues, we report the final computed values as averages over the last 300 ns, taking the standard deviation as a measure of the associated uncertainty. Indeed, while oscillations are still present, the corresponding standard deviation is quite small, even in the less converged cases, resulting in error bars associated with the free energy estimates that are of the same relative magnitude or even less, than the experimental ones.

The computed adsorption free energies are reported and compared to the experimental values in Fig. 7b. As was the case for histidine, a remarkable agreement is also obtained for the other amino acids. The computed value for Ser, -8.9±1.0 kcal mol^{-1}, has the largest residual error that however includes the experimental measurement (-9.6±0.1 kcal mol^{-1}).

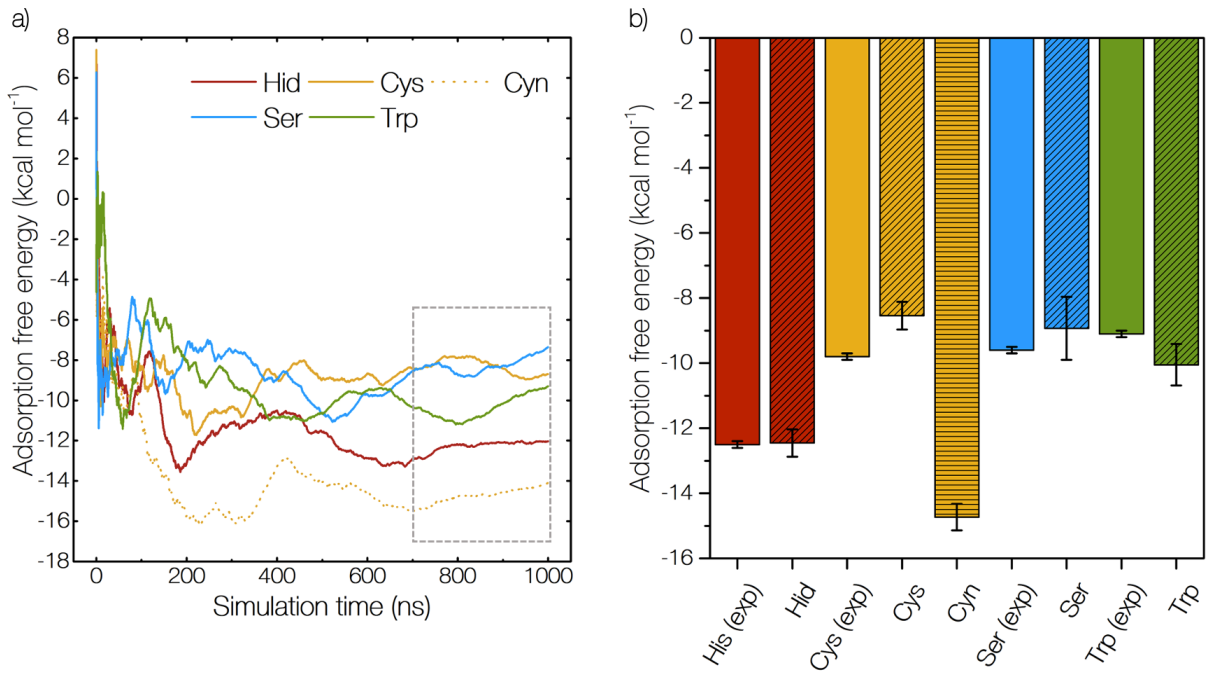

Figure 7: *a) Variation of the adsorption free energy, computed as in Eq. 2, during the REST-MetaD simulation time, for the selected amino acids in methanol. For cystine, also the case with a deprotonated thiol group (Cyn) is reported. The dashed gray rectangle highlights the window in which the final energies were averaged. b) Adsorption free energy for the selected amino acids in methanol, in comparison with the experimental O-IDA values.*

The adsorption for Trp is predicted slightly stronger (-10.0±0.6 kcal mol^{-1}) than in the experiment (-9.1±0.1 kcal mol^{-1}), but well within the standard target for chemical accuracy in computations (1 kcal mol^{-1}). The highest deviation between experiment and calculation was found for the Cys case and was therefore further investigated.

In previous DFTB simulations a surface-mediated chemical reaction was observed for cysteine interacting with the ZnO($10\bar{1}0$) surface in an aqueous environment. This reaction was a proton transfer from the thiol group to a hydroxyl group of the surface hydration layer,[43] which is in good agreement with the binding mode found for Zn^{2+} ions in zinc finger proteins.[60] Since our classical simulation approach is not able to reproduce any chemical reactivity during adsorption, we decided to investigate two different cysteine configurations, namely: Cys, with a thiol group, and Cyn, with a deprotonated thiol group. From our simulations, as reported in Fig. 6b and 7b, we observe a slight underestimation of the binding

free energy for the interaction of Cys (-8.5±0.4 kcal mol^{-1}) and a strong overestimation of the value based on the interaction of Cyn (-14.7±0.4 kcal mol^{-1}) in comparison with the experimental value (-9.8±0.1 kcal mol^{-1}). This divergence is not surprising, since the actual process, with a Cys approaching ZnO and possibly transforming into Cyn upon interaction, is expected to lie in between these two extremes.

As a further comparison, the canonical forms of the amino acids were investigated. The resulting adsorption free energies, however, range between -4.6 (Cys) and -6.9 (Hid) kcal mol^{-1} (Figure S12 in Supporting Information), considerably lower than the experimental values obtained by our O-IDA approach. This disagreement further suggests that the zwitterionic state may be the favored state for the investigated amino acids adsorbing from bulk methanol to the $(10\bar{1}0)$ ZnO surface.

As an additional step towards shedding light on the effect of surface proximity on the protonation state of the adsorbed amino acids, we have taken the closest adsorption configuration of Hid on the surface, as obtained classically, removed bulk methanol leaving only the first solvation layer and performed a full DFT geometry optimization of two situations: one with zwitterionic histidine and one in which a proton from $NH3^+$ has moved to the surface (Figure S13 in Supporting Information). The potential energy difference between these states was computed as 15 kcal mol^{-1}, suggesting that this process is energetically unfavored, with the zwitterionic state preserved after amino acid adsorption at the ZnO/methanol interface. Finally, a short ab initio MD simulation on the same adsorption configuration did not show any hint of a proton transfer from the charged N-terminus.

3.5 Binding modes of amino acids on ZnO $(10\bar{1}0)$

Based on the good agreement between the free energies of experiment and simulation, we can elucidate the binding configurations of the amino acids to gain a more detailed understanding of the driving forces of the interactions. Fig. 8 and Fig. 9 depict the most stable adsorption configurations of the four amino acids, corresponding to the free energy minima identified in

the profiles of Fig. 6. As mentioned before, both Cys and Ser show only one minimum for the adsorbed state, while multiple local minima, i.e. multiple adsorption geometries, emerge for Hid and Trp. In no case are methanol molecules observed to act as bridges between ZnO and the amino acids, with all adsorption configurations close to the surface having direct amino acid/ZnO interactions, stabilized by a methanol solvation shell on the opposite side textcolorred(Figures S14-15 in Supporting Information).

As expected from similar interactions found in zinc finger proteins, in which a Zn^{2+} ion is coordinated by two histidine and two cysteine residues,[60] the main mode of adsorption for Hid (Fig. 8a) is an interaction between the deprotonated δ-N and Zn which is dominant in the global minimum (present in 73% of the frames in the CV range). Interestingly, in most situations (93%) this interaction is accompanied by an interaction between the charged N-terminus and the O atoms of the surface, while only in limited cases (26%) is the C-terminus participating in the interaction with the surface, preferring instead (100%) the solvent above. Remarkably, the second free energy minimum in order of stability (located at about 4.5 Å in Fig. 6a) sees a strong enrichment in C-terminus/Zn interactions (69%) with a concurrent drop in δ-N/Zn binding (2%), suggesting that steric constraints make the simultaneous interaction of both termini and the imidazole ring unlikely (Fig. 8b). Indeed, this simultaneous interaction is observed in the small free energy minimum closest to the surface, that is, however 8 kcal mol^{-1} higher in energy with respect to the global minimum. This local minimum is more prominent in the case of a bare ZnO surface while it disappears at the highest degree of hydroxylation (Fig. 5a), due to a strong dependency on the availability of surface sites. Apart from this local minimum, the protonated ϵ-N of Hid favors instead the interaction with the surface hydroxyls and methanol (Fig. 8b).

The adsorbed state of Cys with protonated side chain (Fig. 8c) is characterized by a hydrogen-bond between the thiol group and the surface hydroxyl groups (66%), together with termini/ZnO interactions (75% and 61% for the N- and C-terminus, respectively). The SH group, on the other hand, only rarely interacts with the underlying Zn or O atoms of

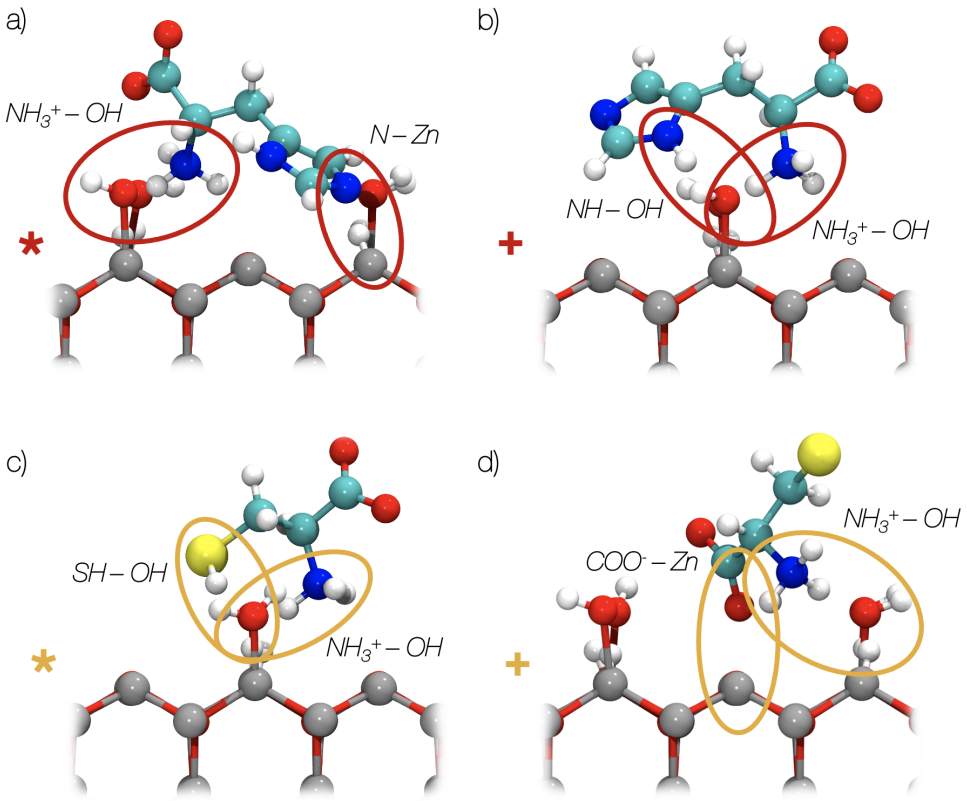

Figure 8: *Exemplary snapshots of the most stable adsorption configurations for the zwitterionic forms of Hid (a-b), Cys (c), Cyn (d) on the ZnO (10$\bar{1}$0) surface in methanol, extracted from the free energy minima identified in the profiles of Fig. 6. Color code as in Fig. 2 and 3. Circles highlights the main interactions.*

the surface (<2%), in contrast to interactions found in zinc finger proteins.[60] The SH/OH interaction was predicted in previous DF-TB simulations[43] carried out in water solvent as the first binding step before a subsequent proton-transfer reaction. Interestingly, in our classical simulations in methanol, a deprotonated thiol group (Cyn) shows almost no interaction (<4%) with either the surface Zn and O atoms or the terminal OH groups (Fig. 8d). Instead, the S atom remains coordinated by multiple methanol molecules and adsorption is driven by both termini interacting with the surface (>90%). It is unclear, however, whether such a flip of the side chain far from the surface would happen after a Cys deprotonation on the surface.

The Ser case (Fig. 9a-b) is quite different from Cys, despite some similarities between the thiol and hydroxyl functionalities. In fact, in the free energy minimum Ser adsorbs via

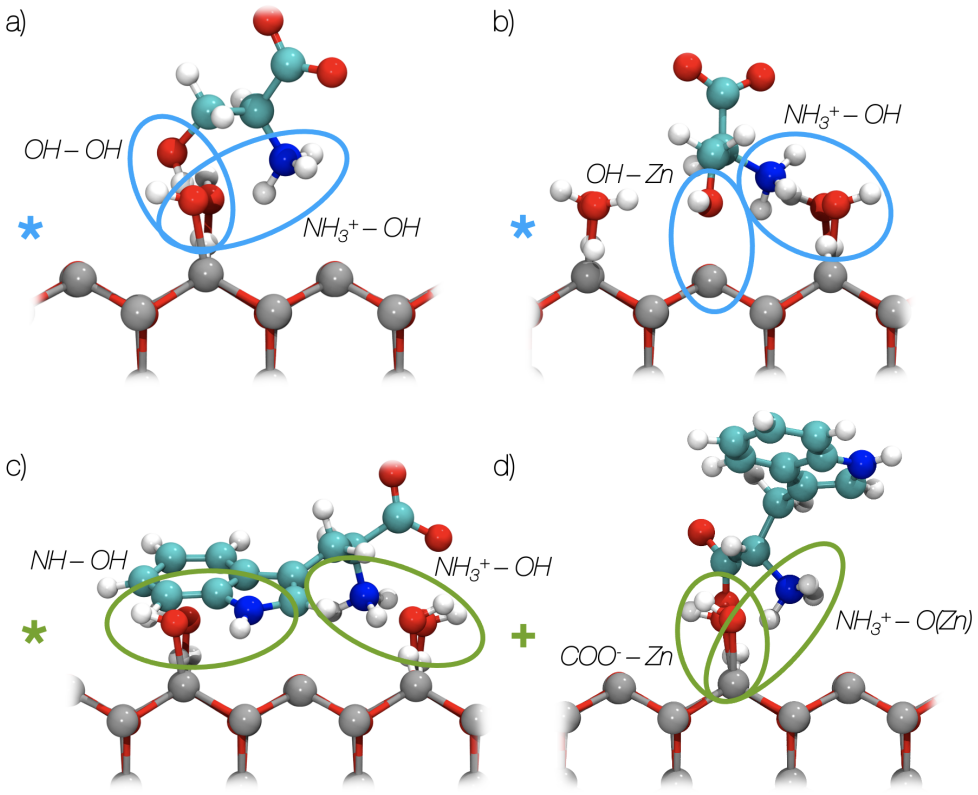

Figure 9: *Exemplary snapshots of the most stable adsorption configurations for the zwitterionic forms of Ser (a-b) and Trp (c-d) on the ZnO (10$\bar{1}$0) surface in methanol, extracted from the free energy minima identified in the profiles of Fig. 6. Color code as in Fig. 2 and 3. Circles highlights the main interactions.*

its side chain to both terminal OH groups (85%, Fig. 9a) and the Zn (66%, Fig. 9b) and O (83%) atoms of the surface, together with a N-terminus/ZnO interaction (94%). As in the Hid case, the C-terminus prefers (99%) the solvent over Zn (1%). The high propensity of Ser for hydrogen bonding with the surface is in agreement with previous quantum mechanical simulations in water, where the adsorption energy was predominately based on the direct or indirect formation of hydrogen bonds, as well as the rearrangement of the hydrogen-bond network in surface proximity in the aqueous system.[43]

Finally, Trp (Fig. 9c-d) is the only case in which the global minimum in free energy sees no interaction between the amino acid's side chain and ZnO, while adsorption is driven solely by both termini interacting with the surface atoms (77% and 97% for the N- and C-terminus, respectively, as in Fig. 9d). Indeed, the NH group of the Trp pyrrole ring undergoes only

hydrogen-bonding (92%) with methanol. However, the situation is switched in the case of the other local adsorption minimum closer to the surface (Fig. 6d), only 2 kcal mol^{-1} higher in energy. Here, binding is instead driven by interactions between the NH group of the pyrrole ring and ZnO (64%), with concurrent N-terminus/ZnO interactions (99%). As in other cases, the simultaneous three-point binding of side chain and both termini is unlikely, with the C-terminus only partly (32%) interacting with the surface (Fig. 9c).

4 Conclusions

Simulating adsorption of amino acids on ZnO in a non-aqueous environment proved to be a surprisingly difficult task, in which several challenges needed to be addressed in order to achieve agreement with experimental measurements.

First of all, we had to develop and validate a novel parameterization of a Coulomb/LJ force field to describe the interactions between ZnO and biomolecules. By doing so, we filled an important gap in the current literature, enabling the study of more complex interfaces of ZnO-based functional biomaterials. Moreover, the parameter set developed for this work can also be straightforwardly coupled to intra-molecular ZnO potentials, if necessary, to describe more complex interface phenomena.

The designed force field is applicable to both aqueous and non-aqueous environments, a prerequisite particularly essential in the ZnO case, because of the dissolution of this material in water.[34] In methanol, on the other hand, non-polar single-crystalline ZnO surfaces such as the here-investigated $(10\bar{1}0)$ facet are stable, which enabled precise experimental estimations of adsorption free energies of single amino acids by means of the O-IDA method.[33] These accurate measurements represented a valuable proving ground to assess our computational approach.

The resulting remarkably good agreement obtained between the experiments and simulations (within the common target for chemical accuracy) was made possible by a careful

understanding of previously unclear features of the ZnO/methanol/amino-acid systems, in particular:

(i) The amino acids are expected to be in a zwitterionic state in the bulk methanol solvent and preserve this state upon adsorption on the surface. This is supported directly by the DFT prediction of the free-energy profile associated with a proton transfer from the COOH to the NH_2 moiety in glycine (Fig. 4) and indirectly by the severely underestimated ΔG_{ads} values obtained for canonical amino acids (cf. Figure S12 in Supporting Information). Additionally, deprotonation of the charged N-terminus by the surface was found energetically unfavored.

(ii) The ZnO $(10\bar{1}0)$ surface is expected to retain a substantial degree of hydroxylation (in the range of 25 % according to our models) when in contact with bulk methanol. The origin of the OH groups could either stem from previous contact of the material with the aqueous environment (e.g. during synthesis or handling in an atmosphere), or from the reaction with water traces in the methanol solution (in which H_2O readily dissolves). This finding is supported by the alignment of ΔG_{ads} obtained for 25% OH coverage as opposed to either the bare surface or higher OH coverage. The predicted values of the heat of immersion are less conclusive in supporting this finding, but we note here that the experimental value is associated with a rather large error bar, within which fall both the heat of immersion values computed for an OH coverage of 25 % and a bare surface. Moreover, the experimental value is strongly dependent on the kind of pre-treatment (in particular heating at a few hundred degrees), which may indeed free the surface from any residual adsorbed H_2O or OH groups. Both classical and DFT simulations suggested that spontaneous methanol dissociation should not take place when the surface is pre-exposed to an aqueous environment and ambient conditions.

From a methodological point of view, this challenging system revealed the absolute importance of explicitly biasing the surface/solvent interactions in the framework of a mixed REST-metaD approach, in which also the Zn and O surface atoms are considered part of the

'solute' along with the adsorbing amino acid. Only in this way the adsorbing molecule can steer frequently enough through the very narrow adsorption channels dictated by the strong methanol structuring in surface proximity, within a reasonable simulation time (of the order of one microsecond).

The simulations allowed us to approach the atomistic origin of the experimental adsorption free energies. The adsorption of the amino acids takes place via direct surface/molecule interactions and is never bridged by the methanol solvent. The latter provides a solvation shell around the adsorbed molecule that stabilizes the adsorbed state. Remarkably, we found that the adsorption of histidine on ZnO follows the same pattern found in zinc finger proteins,[60] while we were not able to observe the same configuration for the cysteine case.

We believe that the knowledge gained and the optimised computational machinery can allow for the set-up of a rational design platform for ZnO-based bio-nanocomposites. More generally, we foresee that the lessons learned on this challenging case can be extended to other complex interfaces, where a delicate balance of physical and chemical processes exists and needs to be addressed in order to model the system. Finally, we show that the availability of accurate experimental measurements can support the development and improvement of the modeling approach and we demonstrated that our recently introduced O-IDA method can fulfill this role, being also easily extendable to more complex biomolecules.

Acknowledgement

MDP and MM contributed equally to this work. This work was supported by the Deutsche Forschungsgemeinschaft under grants CO 1043/17-1 / RO 3965/3-1 and GRK 2247 and received funding from the Air Force Office of Scientific Research (AFOSR) grant FA9550-1-16-0213. DR greatly acknowledges the opportunity to perform research in the department of Prof. Dr. Joachim Bill. Computational resources were provided by the North-German Supercomputing-Alliance (HLRN).

Supporting Information Available

Supporting Information includes: ZnO parameter set (Figure S1); all investigated energy-distance curves for the parametrization (Figures S2-7); model of a ZnO surface after a 50% dissociation of an adsorbed methanol monolayer (Figure S8); DFT molecular dynamics simulations of glycine in water and methanol (Figure S9); comparison between enhanced sampling methods for the computation of adsorption free energies (Figures S10-11); overview of the computed adsorption free energies, including the canonical amino acids (Figure S12); DFT investigation of the energetics of a proton transfer at the interface (Figure S13); snapshots of the most stable adsorption configurations of the amino acids, including the methanol molecules in close proximity (Figures S14-15).

References

(1) Hamley, I. W. Small bioactive peptides for biomaterials design and therapeutics. *Chemical reviews* **2017**, *117*, 14015–14041.

(2) Cai, P.; Zhang, X.; Wang, M.; Wu, Y.-L.; Chen, X. Combinatorial Nano–Bio Interfaces. *ACS Nano* **2018**, *12*, 5078–5084.

(3) Kilper, S.; Jahnke, T.; Aulich, M.; Burghard, Z.; Rothenstein, D.; Bill, J. Genetically Induced In Situ-Poling for Piezo-Active Biohybrid Nanowires. *Advanced Materials* **2019**, *31*, 1805597.

(4) Limo, M. J.; Sola-Rabada, A.; Boix, E.; Thota, V.; Westcott, Z. C.; Puddu, V.; Perry, C. C. Interactions between Metal Oxides and Biomolecules: from Fundamental Understanding to Applications. *Chemical Reviews* **2018**, *118*, 11118–11193.

(5) Brown, S. Metal-recognition by repeating polypeptides. *Nature Biotechnology* **1997**, *15*, 269.

(6) Willett, R.; Baldwin, K.; West, K.; Pfeiffer, L. Differential adhesion of amino acids to inorganic surfaces. *Proceedings of the National Academy of Sciences* **2005**, *102*, 7817–7822.

(7) Wu, Q.; Chen, X.; Zhang, P.; Han, Y.; Chen, X.; Yan, Y.; Li, S. Amino Acid-Assisted Synthesis of ZnO Hierarchical Architectures and Their Novel Photocatalytic Activities. *Crystal Growth & Design* **2008**, *8*, 3010–3018.

(8) Costa, D.; Savio, L.; Pradier, C.-M. Adsorption of Amino Acids and Peptides on Metal and Oxide Surfaces in Water Environment: A Synthetic and Prospective Review. *The Journal of Physical Chemistry B* **2016**, *120*, 7039–7052, PMID: 27366959.

(9) Heinz, H.; Ramezani-Dakhel, H. Simulations of inorganic–bioorganic interfaces to discover new materials: insights, comparisons to experiment, challenges, and opportunities. *Chem. Soc. Rev.* **2016**, *45*, 412–448.

(10) Scarano, D.; Spoto, G.; Bordiga, S.; Zecchina, A.; Lamberti, C. Lateral interactions in CO adlayers on prismatic ZnO faces: a FTIR and HRTEM study. *Surface Science* **1992**, *276*, 281 – 298.

(11) Özgür, Ü.; Alivov, Y. I.; Liu, C.; Teke, A.; Reshchikov, M.; Doğan, S.; Avrutin, V.; Cho, S.-J.; Morkoc, H. A comprehensive review of ZnO materials and devices. *Journal of Applied Physics* **2005**, *98*, 11.

(12) Piccinno, F.; Gottschalk, F.; Seeger, S.; Nowack, B. Industrial production quantities and uses of ten engineered nanomaterials in Europe and the world. *Journal of Nanoparticle Research* **2012**, *14*, 1109.

(13) Brif, A.; Ankonina, G.; Drathen, C.; Pokroy, B. Bio-Inspired Band Gap Engineering of Zinc Oxide by Intracrystalline Incorporation of Amino Acids. *Advanced Materials* **2014**, *26*, 477–481.

(14) Muhammed, M. A. H.; Lamers, M.; Baumann, V.; Dey, P.; Blanch, A. J.; Polishchuk, I.; Kong, X.-T.; Levy, D.; Urban, A. S.; Govorov, A. O.; Pokroy, B.; Rodríguez-Fernández, J.; Feldmann, J. Strong Quantum Confinement Effects and Chiral Excitons in Bio-Inspired ZnO–Amino Acid Cocrystals. *The Journal of Physical Chemistry C* **2018**, *122*, 6348–6356.

(15) Guo, Y.; Lin, S.; Li, X.; Liu, Y. Amino acids assisted hydrothermal synthesis of hierarchically structured ZnO with enhanced photocatalytic activities. *Applied Surface Science* **2016**, *384*, 83 – 91.

(16) Liang, M.-K.; Limo, M. J.; Sola-Rabada, A.; Roe, M. J.; Perry, C. C. New Insights into the Mechanism of ZnO Formation from Aqueous Solutions of Zinc Acetate and Zinc Nitrate. *Chemistry of Materials* **2014**, *26*, 4119–4129.

(17) Ponder, J. W.; Case, D. A. *Advances in protein chemistry*; Elsevier, 2003; Vol. 66; pp 27–85.

(18) Lopes, P. E.; Guvench, O.; MacKerell, A. D. *Molecular modeling of proteins*; Springer, 2015; pp 47–71.

(19) Heinz, H.; Lin, T.-J.; Kishore Mishra, R.; Emami, F. S. Thermodynamically Consistent Force Fields for the Assembly of Inorganic, Organic, and Biological Nanostructures: The INTERFACE Force Field. *Langmuir* **2013**, *29*, 1754–1765, PMID: 23276161.

(20) Wright, L. B.; Rodger, P. M.; Walsh, T. R.; Corni, S. First-Principles-Based Force Field for the Interaction of Proteins with Au(100)(5×1): An Extension of GolP-CHARMM. *The Journal of Physical Chemistry C* **2013**, *117*, 24292–24306.

(21) Butenuth, A.; Moras, G.; Schneider, J.; Koleini, M.; Köppen, S.; Meißner, R.; Wright, L. B.; Walsh, T. R.; Ciacchi, L. C. Ab initio derived force-field parameters for molecular dynamics simulations of deprotonated amorphous-SiO2/water interfaces. *physica status solidi (b)* **2012**, *249*, 292–305.

(22) Schneider, J.; Ciacchi, L. C. A Classical Potential to Model the Adsorption of Biological Molecules on Oxidized Titanium Surfaces. *Journal of Chemical Theory and Computation* **2011**, *7*, 473–484, PMID: 26596167.

(23) Larrucea, J.; Lid, S.; Colombi Ciacchi, L. Parametrization of a classical force field for iron oxyhydroxide/water interfaces based on Density Functional Theory calculations. *Computational Materials Science* **2014**, *92*, 343–352.

(24) Lid, S.; Köppen, S.; Colombi Ciacchi, L. Creation of models and parametrization of a classical force field for amorphous Al2O3/water interfaces based on Density Functional Theory. *Computational Materials Science* **2017**, *140*, 307–314.

(25) Schneider, J.; Colombi Ciacchi, L. Specific material recognition by small peptides mediated by the interfacial solvent structure. *Journal of the American Chemical Society* **2012**, *134*, 2407–2413.

(26) Xu, Z.; Yang, X.; Wei, Q.; Zhao, W.; Cui, B.; Yang, X.; Sahai, N. Quantitatively Identifying the Roles of Interfacial Water and Solid Surface in Governing Peptide Adsorption. *Langmuir* **2018**, *34*, 7932–7941, PMID: 29888924.

(27) Nawrocki, G.; Cieplak, M. Amino acids and proteins at ZnO-water interfaces in molecular dynamics simulations. *Physical Chemistry Chemical Physics* **2013**, *15*, 13628–13636.

(28) Quaranta, V.; Behler, J.; Hellström, M. Structure and Dynamics of the Liquid–Water/Zinc-Oxide Interface from Machine Learning Potential Simulations. *The Journal of Physical Chemistry C* **2019**, *123*, 1293–1304.

(29) Bernardi, R. C.; Melo, M. C.; Schulten, K. Enhanced sampling techniques in molecular dynamics simulations of biological systems. *Biochimica et Biophysica Acta (BBA) - General Subjects* **2015**, *1850*, 872–877, Recent developments of molecular dynamics.

(30) Wei, Q.; Zhao, W.; Yang, Y.; Cui, B.; Xu, Z.; Yang, X. Method Evaluations for Adsorption Free Energy Calculations at the Solid/Water Interface through Metadynamics, Umbrella Sampling, and Jarzynski's Equality. *ChemPhysChem* **2018**, *19*, 690–702.

(31) Comitani, F.; Gervasio, F. L. Exploring cryptic pockets formation in targets of pharmaceutical interest with SWISH. *Journal of chemical theory and computation* **2018**, *14*, 3321–3331.

(32) Bhakat, S.; Söderhjelm, P. Resolving the problem of trapped water in binding cavities: prediction of host–guest binding free energies in the SAMPL5 challenge by funnel metadynamics. *Journal of computer-aided molecular design* **2017**, *31*, 119–132.

(33) Michaelis, M.; Fayyaz, A.; Parambath, M.; Koeppen, S.; Ciacchi, L. C.; Hanley, Q. S.; Perry, C. C. Platform for Screening Abiotic/Biotic Interactions Using Indicator Displacement Assays. *Langmuir* **2019**, *35*, 14230–14237, PMID: 31609123.

(34) Michaelis, M.; Fischer, C.; Colombi Ciacchi, L.; Luttge, A. Variability of zinc oxide dissolution rates. *Environmental Science & Technology* **2017**, *51*, 4297–4305.

(35) Kresse, G.; Furthmüller, J. Efficient iterative schemes for ab initio total-energy calculations using a plane-wave basis set. *Phys. Rev. B* **1996**, *54*, 11169–11186.

(36) Kresse, G.; Joubert, D. From ultrasoft pseudopotentials to the projector augmented-wave method. *Phys. Rev. B* **1999**, *59*, 1758–1775.

(37) Perdew, J. P.; Burke, K.; Ernzerhof, M. Generalized Gradient Approximation Made Simple. *Phys. Rev. Lett.* **1996**, *77*, 3865–3868.

(38) Grimme, S.; Antony, J.; Ehrlich, S.; Krieg, H. A consistent and accurate ab initio parametrization of density functional dispersion correction (DFT-D) for the 94 elements H-Pu. *The Journal of Chemical Physics* **2010**, *132*, 154104.

(39) Grimme, S. Semiempirical GGA-type density functional constructed with a long-range dispersion correction. *Journal of Computational Chemistry* **2006**, *27*, 1787–1799.

(40) Cutini, M.; Maschio, L.; Ugliengo, P. Exfoliation Energy of Layered Materials by DFT-D: Beware of Dispersion! *Journal of Chemical Theory and Computation* **2020**, *16*, 5244–5252, PMID: 32609519.

(41) Tkatchenko, A.; Scheffler, M. Accurate Molecular Van Der Waals Interactions from Ground-State Electron Density and Free-Atom Reference Data. *Phys. Rev. Lett.* **2009**, *102*, 073005.

(42) große Holthaus, S.; Köppen, S.; Frauenheim, T.; Colombi Ciacchi, L. Atomistic Simulations of the ZnO (1210)/Water Interface: A Comparison between First-Principles, Tight-Binding, and Empirical Methods. *Journal of chemical theory and computation* **2012**, *8*, 4517–4526.

(43) große Holthaus, S.; Köppen, S.; Frauenheim, T.; Ciacchi, L. C. Molecular dynamics simulations of the amino acid-ZnO (10-10) interface: A comparison between density functional theory and density functional tight binding results. *The Journal of Chemical Physics* **2014**, *140*, 234707.

(44) Meyer, B.; Rabaa, H.; Marx, D. Water adsorption on ZnO (1010): from single molecules to partially dissociated monolayers. *Physical Chemistry Chemical Physics* **2006**, *8*, 1513–1520.

(45) Hutter, J.; Iannuzzi, M.; Schiffmann, F.; VandeVondele, J. cp2k: atomistic simulations of condensed matter systems. *WIREs Computational Molecular Science* **2014**, *4*, 15–25.

(46) Bussi, G.; Donadio, D.; Parrinello, M. Canonical Sampling through Velocity Rescaling. *The Journal of Chemical Physics* **2007**, *126*, 014101.

(47) Huang, J.; Rauscher, S.; Nawrocki, G.; Ran, T.; Feig, M.; de Groot, B. L.; Grubmüller, H.; MacKerell Jr, A. D. CHARMM36m: an improved force field for folded and intrinsically disordered proteins. *Nature methods* **2017**, *14*, 71.

(48) Gale, J. D.; Rohl, A. L. The General Utility Lattice Program (GULP). *Molecular Simulation* **2003**, *29*, 291–341.

(49) Pronk, S.; Pall, S.; Schulz, R.; Larsson, P.; Bjelkmar, P.; Apostolov, R.; Shirts, M. R.; Smith, J. C.; Kasson, P. M.; van der Spoel, D.; et al., GROMACS 4.5: a High-Throughput and Highly Parallel Open Source Molecular Simulation Toolkit. *Bioinformatics* **2013**, *29*, 845–854.

(50) Vanommeslaeghe, K.; Hatcher, E.; Acharya, C.; Kundu, S.; Zhong, S.; Shim, J.; Darian, E.; Guvench, O.; Lopes, P.; Vorobyov, I.; Mackerell Jr., A. D. CHARMM general force field: A force field for drug-like molecules compatible with the CHARMM all-atom additive biological force fields. *Journal of Computational Chemistry* **2010**, *31*, 671–690.

(51) Fischer, N. M.; van Maaren, P. J.; Ditz, J. C.; Yildirim, A.; van der Spoel, D. Properties of Organic Liquids when Simulated with Long-Range Lennard-Jones Interactions. *Journal of Chemical Theory and Computation* **2015**, *11*, 2938–2944, PMID: 26575731.

(52) Hess, B. P-LINCS: A Parallel Linear Constraint Solver for Molecular Simulation. *Journal of Chemical Theory and Computation* **2008**, *4*, 116–122, PMID: 26619985.

(53) Humphrey, W.; Dalke, A.; Schulten, K. VMD: Visual Molecular Dynamics. *Journal of Molecular Graphics* **1996**, *14*, 33–38.

(54) Barducci, A.; Bussi, G.; Parrinello, M. Well-Tempered Metadynamics: A Smoothly Converging and Tunable Free-Energy Method. *Physical Review Letters* **2008**, *100*.

(55) Bonomi, M.; Branduardi, D.; Bussi, G.; Camilloni, C.; Provasi, D.; Raiteri, P.; Donadio, D.; Marinelli, F.; Pietrucci, F.; Broglia, R. A.; Parrinello, M. PLUMED: A portable

plugin for free-energy calculations with molecular dynamics. *Computer Physics Communications* **2009**, *180*, 1961 – 1972.

(56) Tribello, G. A.; Bonomi, M.; Branduardi, D.; Camilloni, C.; Bussi, G. PLUMED 2: New feathers for an old bird. *Computer Physics Communications* **2014**, *185*, 604 – 613.

(57) Affentranger, R.; Tavernelli, I.; Di Iorio, E. E. A novel Hamiltonian replica exchange MD protocol to enhance protein conformational space sampling. *Journal of chemical theory and computation* **2006**, *2*, 217–228.

(58) Wang, L.; Friesner, R. A.; Berne, B. J. Replica Exchange with Solute Scaling: a More Efficient Version of Replica Exchange with Solute Tempering (REST2). *The Journal of Physical Chemistry B* **2011**, *115*, 9431–9438.

(59) Bussi, G. Hamiltonian replica exchange in GROMACS: a flexible implementation. *Molecular Physics* **2013**, *112*, 379–384.

(60) Dudev, T.; Lim, C. Principles governing Mg, Ca, and Zn binding and selectivity in proteins. *Chemical Reviews* **2003**, *103*, 773–788.

(61) Rothenstein, D.; Claasen, B.; Omiecienski, B.; Lammel, P.; Bill, J. Isolation of ZnO-binding 12-mer peptides and determination of their binding epitopes by NMR spectroscopy. *Journal of the American Chemical Society* **2012**, *134*, 12547–12556.

(62) Raymand, D.; van Duin, A. C.; Spångberg, D.; Goddard III, W. A.; Hermansson, K. Water adsorption on stepped ZnO surfaces from MD simulation. *Surface Science* **2010**, *604*, 741–752.

(63) Maret, W.; Li, Y. Coordination dynamics of zinc in proteins. *Chemical reviews* **2009**, *109*, 4682–4707.

(64) Liao, S.-M.; Du, Q.-S.; Meng, J.-Z.; Pang, Z.-W.; Huang, R.-B. The multiple roles of histidine in protein interactions. *Chemistry Central Journal* **2013**, *7*, 44.

(65) Daniel, A. G.; Farrell, N. P. The dynamics of zinc sites in proteins: electronic basis for coordination sphere expansion at structural sites. *Metallomics* **2014**, *6*, 2230–2241.

(66) Horinek, D.; Serr, A.; Geisler, M.; Pirzer, T.; Slotta, U.; Lud, S.; Garrido, J.; Scheibel, T.; Hugel, T.; Netz, R. Peptide adsorption on a hydrophobic surface results from an interplay of solvation, surface, and intrapeptide forces. *Proceedings of the National Academy of Sciences* **2008**, *105*, 2842–2847.

(67) Dulub, O.; Meyer, B.; Diebold, U. Observation of the dynamical change in a water monolayer adsorbed on a ZnO surface. *Physical review letters* **2005**, *95*, 136101.

(68) Kiss, J.; Langenberg, D.; Silber, D.; Traeger, F.; Jin, L.; Qiu, H.; Wang, Y.; Meyer, B.; Wöll, C. Combined Theoretical and Experimental Study on the Adsorption of Methanol on the ZnO (1010) Surface. *The Journal of Physical Chemistry A* **2011**, *115*, 7180–7188.

(69) Shao, X.; Fukui, K.-i.; Kondoh, H.; Shionoya, M.; Iwasawa, Y. STM study of surface species formed by methanol adsorption on stoichiometric and reduced ZnO (10-10) surfaces. *The Journal of Physical Chemistry C* **2009**, *113*, 14356–14362.

(70) Morimoto, T.; Nagao, M.; Hirata, M. The heat of immersion of zinc oxide in water. *Kolloid-Zeitschrift und Zeitschrift für Polymere* **1968**, *225*, 29–33.

(71) Sakurai, T.; Okabe, H.; Isoda, T. Heat of Immersion of Zinc Oxide. *Bulletin of The Japan Petroleum Institute* **1970**, *12*, 142–145.

(72) Tuñón, I.; Silla, E.; Ruiz-López, M. F. On the tautomerization process of glycine in aqueous solution. *Chemical Physics Letters* **2000**, *321*, 433 – 437.

(73) Tolosa, S.; Hidalgo, A.; Sansón, J. A. Amino Acid Tautomerization Reactions in Aqueous Solution via Concerted and Assisted Mechanisms Using Free Energy Curves from

MD Simulation. *The Journal of Physical Chemistry B* **2012**, *116*, 13033–13044, PMID: 23072511.

(74) Meißner, R. H.; Schneider, J.; Schiffels, P.; Colombi Ciacchi, L. Computational Prediction of Circular Dichroism Spectra and Quantification of Helicity Loss upon Peptide Adsorption on Silica. *Langmuir* **2014**, *30*, 3487–3494, PMID: 24627945.

(75) Hildebrand, N.; Michaelis, M.; Wurzler, N.; Li, Z.; Hirst, J. D.; Micsonai, A.; Kardos, J.; Gil-Ley, A.; Bussi, G.; Köppen, S.; Delle Piane, M.; Ciacchi, L. C. Atomistic Details of Chymotrypsin Conformational Changes upon Adsorption on Silica. *ACS Biomaterials Science & Engineering* **2018**, *4*, 4036–4050, PMID: 33418804.

For table of contents only